Chemical composition and phase identification of sodium titanate nanostructures grown from titania by hydrothermal processing

R.A. Zárate[a,*], S. Fuentes[a], J.P. Wiff[b,1], V.M. Fuenzalida[b], A.L. Cabrera[c]

[a]*Departamento de Física, Facultad de Ciencias, Universidad Católica del Norte, Casilla 1280, Antofagasta, Chile*
[b]*Departamento de Física, Facultad de Ciencias Físicas y Matemáticas, Universidad de Chile, Casilla 487-3, Santiago, Chile*
[c]*Facultad de Física, Pontificia Universidad Católica de Chile, Casilla 306, Santiago 22, Chile*

Abstract

Fine titanium dioxide particles were hydrothermally treated in a sodium hydroxide aqueous solution. The treatment extended from 1 to 6 days leading to belt-like and wire-like structures of a metastable phase of sodium titanate, with typical widths and diameters between 8 and 40 nm, and lengths from 100 nm to several micrometers. These conclusions are supported by X-ray photoelectron spectroscopy, X-ray diffraction, Raman spectroscopy and high resolution transmission electron microscopy. The latter method revealed two set of space fringes with characteristic distances of 0.29 and 0.34 nm. These distances could correspond to the lattice spacing of [−3 1 1] and [−1 1 1] planes in $Na_2Ti_6O_{13}$ compounds. The nanomaterial was found to be stable up to temperatures as high as 200 or 400 °C depending on the reaction time and the concentration.

Keywords: C. X-ray diffraction

1. Introduction

Materials with different structures at the nanometer scale, such as grains, dots, ribbons, tubes and wires may have a conspicuous impact on future advanced technology [1–3]. Alkaline titanates have attracted increasing attention [4–7], particularly for the applications based on their high photocatalytic activity, such as fuel cell electrolytes, cation exchangers for the treatment of radioactive liquid waste [8,9], and many other applications [10–13].

The standard method for the preparation of sodium titanate consists of the reaction of TiO_2 with fused Na_2CO_3 at temperatures around 1000 °C [14]; the typical particle size of the products obtained is about 50 μm. Sol–gel methods [5] have also been used to synthesize sodium titanate, with particle size around 10 μm. Structures with much smaller features have been synthesized by Kasuga et al. [15] using a simple hydrothermal process. Their procedure was to mix fine TiO_2 particles (rutile or anatase phase) and aqueous NaOH solution in a sealed reactor at 100−160 °C, followed by a treatment in 0.1 M HCl. This led to tubular structures with diameters about 10 nm and lengths around 100 nm. They concluded that the nanotubes were formed during the post treatment with 0.1 M HCl.

After Kasuga [15], there has been a particular interest in the hydrothermal method to obtain TiO_2-derived nanotubes due to the large surface area of the products and the relative simple way to the large scale synthesis of nanotubes or nanowires in a one single reaction [16]. However, the literature shows disperse results: the crystalline phase of the as-synthesized products is still a controversy. After treating pure TiO_2 in a NaOH solution, several groups reported the synthesis of TiO_2 [15,17–23], others have reported that their products exhibited a monoclinic crystallographic phase $H_2Ti_3O_7$ [24–29]. The phases $H_2Ti_2O_4(OH)_2$ or $Na_2Ti_2O_4(OH)_2$ have also been reported [6,30–34]. Other researchers have assigned the XRD reflections to the orthorhombic lepidocrocite type phases

*Corresponding author. Tel.: +56 55 355517; fax: +56 55 355521.
E-mail address: rzarate@ucn.cl (R.A. Zárate).
[1]Present address: Nagaoka University of Technology, Mat. Sci. Lab., Nagaoka, Niigata 940-2188, Japan.

$H_{0.7}Ti_{1.855}\square_{0.175}O_{4.0}H_2O$ [35,36], where the square represents an oxygen vacancy, or $Na_2Ti_3O_7 \cdot nH_2O$ phase [37] or hydrogen sodium titanate [38].

Recently, Poudel et al. [39] obtained highly crystallized titania nanotubes, which depended on the filling volume fraction of the autoclave as well as the concentration of the acid treatment. These parameters were found to be critical to the control of crystallinity and purity. Seo et al. [40] synthesized $Na_2Ti_6O_{13}$ whiskers hydrothermally, which led to TiO_2 whiskers after a treatment in 0.5 M HCl at 100 °C for 48 h. Wei et al. [41] started with layered $Na_2Ti_3O_7$ particles which, after a treatment in deionized water at 140−170 °C for 5–18 days, led to TiO_2 nanotubes. On the other hand, Kukovez et al. [42] indicated that the precursor $Na_2Ti_3O_7$ is not destroyed by the NaOH solution, and therefore recrystallization into nanotubes does not occur.

We used a modified Kasuga process, which originates the synthesis of sodium titanate nanostructures instead of the TiO_2-derived nanotubes reported in the literature [15,17–23]. In this paper we report on the structural evolution and chemical properties of the synthesized products, and their correlation with the synthesis parameters. Although several previous articles used the XPS technique [6,43,44], our emphasis is correlating it with Raman spectroscopy, XRD and HRTEM observations in order to elucidate the existence of Na^+-O-Ti bonds, following the procedure of Ref. [45].

2. Experimental

All precursors were of analytical grade, obtained from Aldrich: titanium (IV) oxide powder (99.8% pure) in the anatase phase and pellets of sodium hydroxide (99.99% pure).

Sodium titanate was prepared as follows: 25 ml of a NaOH aqueous solution and 0.21 g of TiO_2 were placed in a Teflon beaker. The mixture was stirred for 1 h at room temperature. The Teflon beaker was placed in the autoclave and heated up to 130 °C for a given period. Several batches were prepared with NaOH solutions of 5 or 10 M and treatment times of 1, 2, 3 and 6 days. After the hydrothermal treatment, the reactor was allowed to cool down to room temperature and the reaction products were removed from the beaker and washed with 0.1 M HCl aqueous solution, and later with water until no acid reaction was detected, to be subsequently filtered and dried at 60 °C.

The sample surface was analyzed by X-ray photoelectron spectroscopy (XPS, Physical Electronics system model 1257), using either Al or Mg K-α emission. Binding energies and oxidation states were obtained from high resolution scans, assigning 284.5 eV to the C 1s peak.

The crystal structure of the powders was obtained from X-ray diffraction in θ-2θ scans (Siemens D5000 powder diffractometer using Cu K-α radiation at 40 kV, 30 mA, non monochromatized).

Additional information was also obtained from Raman spectroscopy (LabRam 010 instrument from ISA-Horiba). A He–Ne laser without filter (633 nm) operated at 5.5 mW was used in these measurements.

Sample morphology was examined with a low vacuum scanning electron microscope (LV-SEM, JSM-5900LV) with X-ray microanalysis capability and a field emission scanning electron microscope (FEG-SEM JSM-6330F). High resolution images were obtained by using a transmission electron microscope (JEOL TEM 3010) operating at 300 kV with spatial resolution of 0.17 nm. This TEM is also equipped with energy dispersive X-ray Spectroscopy (EDX) and selected area electron diffraction (SAED). The samples were dispersed in alcohol using an ultrasonic bath and then trapped on the microscope grid.

Table 1
Binding energy, kinetic energy of Auger lines, energy split of O1s line, and nominal surface atomic percentages (%) of the hydrothermal samples

Sample	Binding energy			Kinetic energy and Auger parameter				Delta	Atomic percentage (%)		
	Ti2p	O1s	Na1s	TiLMM K.E.	α_Ti	OKLL K.E.	α_O	Δ O1s	Ti2p	O1s	Na1s
1 day 5 M	458.4	529.8	1071.1	414.7	873.1	511.9	1041.6	1.9	18	76	6
		531.7				508.8	1040.6				
2 days 5 M	458.4	529.9		414.1	872.4	512.1	1041.8	1.6			
		531.5				508.6	1039.1				
1 day 10 M	458.3	530.0	1071.4	413.7	872.0	511.7	1041.7	1.5	17	73	10
		531.5				508.0	1039.0				
6 days 10 M	458.4	529.7		414.0	872.4	512.1	1041.8	1.6			
		531.2				509.1	1040.3				
Mixture	458.0	529.2	1070.9	414.5	872.5	512.8	1041.3	2.4			
		531.6				508.9	1040.5				
TiO_2	458.0	529.3		415.4	873.4	513.4	1042.6	3.5			
NaOH		532.8	1072.8			508.2	1041.0				
$Na_2Ti_6O_{13}$									28	62	10
$Na_2Ti_3O_7$									25	58	17
$Na_2Ti_2O_5 \cdot H_2O$									17	50	16

3. Results and discussions

3.1. Compositional analysis

3.1.1. Binding energy data

The XPS lines of an insulating sample can shift to higher energies and broaden because of surface charging effects. In this paper the energy scale was fixed by assigning the value of 284.5 eV to the C1s peak. All binding energies were obtained from high-resolution XPS spectra, fitted with standard procedures, leading to the results shown in Table 1.

The O1s photoemission signal of each sample splits in two peaks, the first at 529.7 ± 0.3 eV, attributed to oxygen in titanium dioxide and the second at an energy of 531.5 eV, which is 1.8 ± 0.2 eV higher, attributed to OH groups. The photoemission from oxygen in water is located at a higher binding energy, around 533.2 eV [46], hence we do not attribute the peak at 531.5 eV to adsorbed water on the surface. XPS spectra from a physical mixture of TiO_2 and NaOH were also recorded (Fig. 1), where the O1s line exhibits two peaks separated by 2.4 eV, attributed to different chemical environment of oxygen in both compounds. This value is larger than the splitting of 1.8 ± 0.2 eV measured in our samples, and therefore we conclude that the splitting of the O1s line is not due to residual NaOH, but to the existence of Na^+-O-Ti bonds.

3.1.2. Auger parameter

The Auger parameter α, widely used in surface analysis of mixed oxides [47], is defined as

$$\alpha = h\nu - OKL_{23}L_{23} + O1s,$$

where $OKL_{23}L_{23}$ is the line position of the indicated oxygen Auger line, O1s is the photoemission peak, and the $h\nu - OKL_{23}L_{23}$ is the kinetic energy (KE) of the Auger electron from oxygen. When these lines split in two peaks, there are two Auger parameters for the same sample. Since each spectrum suffers shifts in the same amount, the Auger parameter should not depend on the charging effects or the procedure used to fix the energy scale, although some subtle dependence on charging effects has been reported [48]. The Auger parameter is shown in Table 1.

Fig. 1 shows the Wagner plot (kinetic vs. binding energy) for oxygen corresponding to hydrothermal samples prepared at 5 M for 1 day (empty squares), 5 M for 2 days (filled squares), 10 M for 1 day (empty triangles) and 10 M for 6 days (solid triangles). For comparison we provide data for a physical mixture of TiO_2 and NaOH, recorded under similar conditions (empty circles). Additionally, also for comparison, we have included XPS data in the O 1s and Auger lines of TiO_2 and NaOH (solid circles), which were obtained from the literature [46,55]. The oblique lines (of constant Auger parameter) represent similar chemical states [46]. The mixture did not undergo a hydrothermal treatment, so that the Na^+-O-Ti bond should not exist.

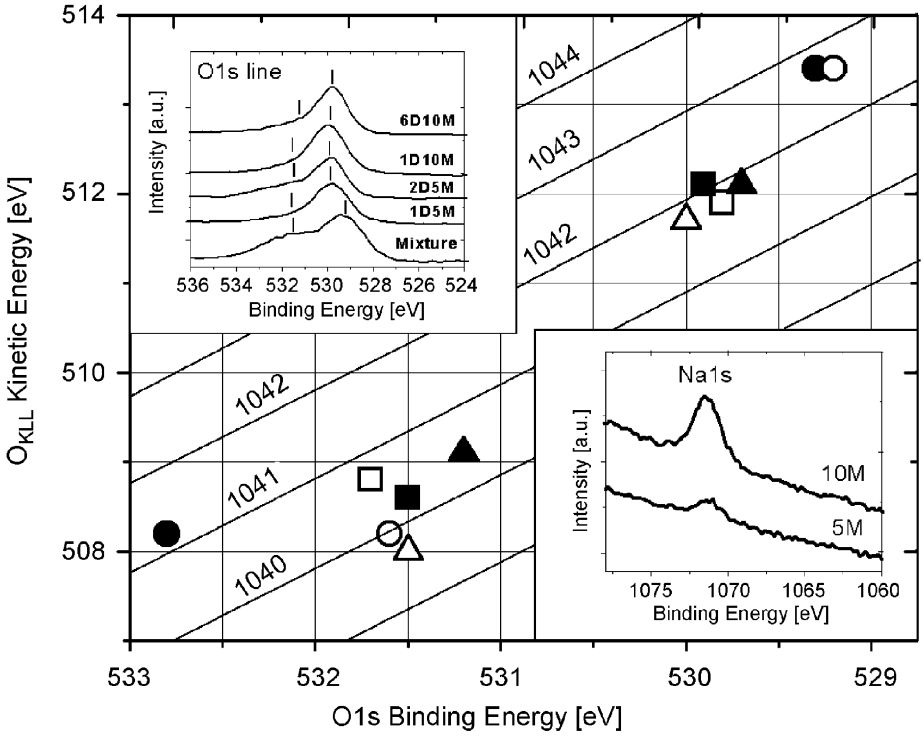

Fig. 1. Wagner plot of the hydrothermal samples treated at (□) 5 M by 1 day, (■) 5 M by 2 days, (△) 10 M by 1 day, and (▲) 10 M by 6 days. The points labeled by (○) correspond to the physical mixture and those labeled by (●) correspond to XPS data of NaOH and TiO_2 obtained from literature. The bottom inset shows high resolution scans of the Na1s line. The top inset is the evolution of O1s peak of the samples.

Each sample synthesized in this work possesses two Auger parameters. The plot shows that the points cluster on two regions on different diagonals, indicating two different chemical environments present in all samples. The points of the XPS data of TiO_2 and NaOH (solid circles) as well as the points of the physical mixture (empty circles) are not on these diagonals. However, the points associated with TiO_2 are coincident for both sources of XPS data, while the other points associated to NaOH are different. We believe that the physical mixture is different because of the unavoidable presence of some water. These points were different to the hydrothermally treated samples, indicating that the chemical environment of oxygen in the physical mixture and in the hydrothermal samples is different. This is consistent with the existence of $Na^{+}-O-Ti$ bonds in the hydrothermal samples, which is absent in the physical mixture [45].

Li et al. [43] investigated how to enhance the thermal stability of mesoporous titania doped with Na_2O by hydrolysis and subsequently aged at room temperature for 1 day and at 80 °C for 5 days. Their XPS results are in agreement with our work, i.e., their samples exhibited shifts toward higher binding energies in the Ti 2p line and toward lower binding energies in the Na 1s line. Finally, their XRD patterns confirmed the formation of sodium hexatitanate (main peaks at $2\theta = 11.84°$, 24.5° and 48.3°). Khan et al. [44] found a shift of 0.8 eV in the Ti 2p line to higher binding energies with respect to pure TiO_2 in powder, which was attributed to the formation of a Ti^{+4}:O^{-2} complex. The shift in the Ti 2p line was larger than in our work, probably because their hydrothermal process and post treatment (samples treated in a H_2O_2 ambient at 40 °C by 4 h) were different to ours.

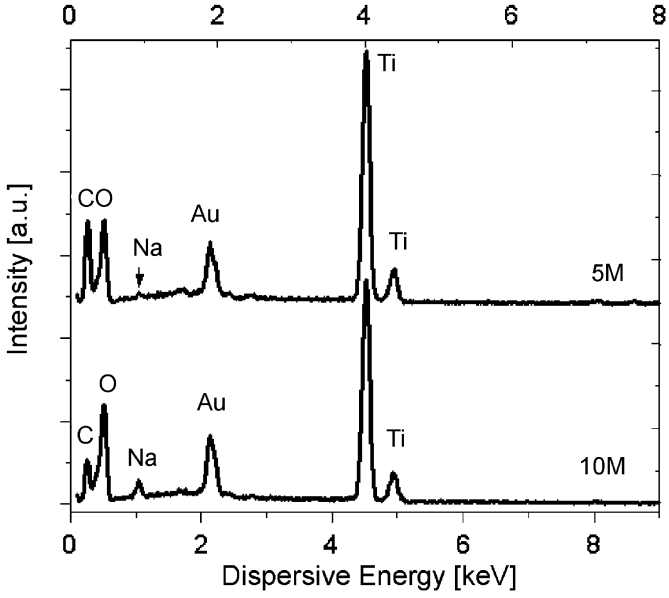

Fig. 2. EDX spectra of hydrothermally-treated samples prepared for 1 day at 130 °C in NaOH solution: 5 M (top curve) and 10 M (bottom curve). The Au line is from gold deposited to make the sample conductive.

3.1.3. Energy dispersive X-ray spectroscopy

Energy dispersive X-ray spectroscopy (EDX) attached to the low vacuum SEM was used to confirm the existence of Na in the hydrothermally treated samples. Fig. 2 shows EDX spectra of the samples treated at both concentrations for 1-day. Both measurements identify C, O, Na, Ti and Au, the latter from the thin Au coating used to improve the electrical conductivity of the samples. Sodium was detected in both samples, treated either at 5 or 10 M NaOH. The Na atomic percentage in the 5 M samples is lower than in the 10 M samples, showing that the Na retention in the TiO_2 matrix was not efficient at low concentration and short reaction times and that residual Na is eliminated in the washing process with HCl. The results shown in Fig. 2 were collected using a magnification of ×80.000, but similar results were found by imaging a bunch of tubular structures at low magnification (×2000). Observation of Na by EDX has been the subject of controversy in the past. Several reports have ignored or not detected Na [19,21,24]. In our case we performed independent measurements of the Na content, using EDX and XPS. The results of both techniques agree with each other.

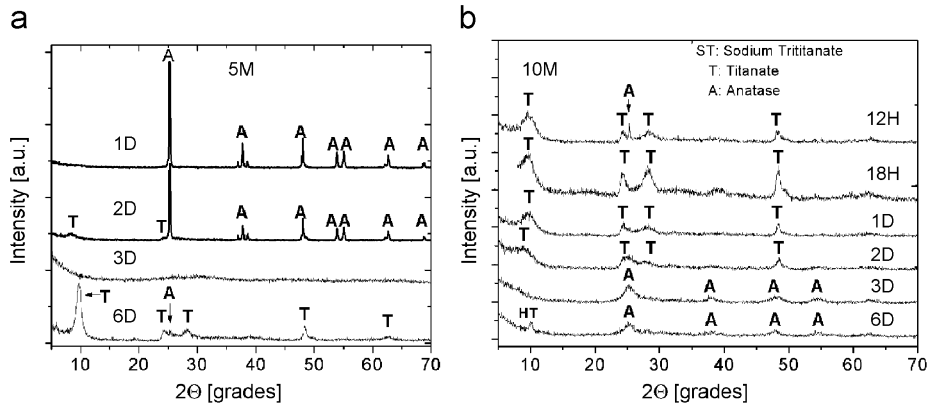

Fig. 3. Evolution of the XRD patterns as a function of the reaction time of hydrothermal samples treated at (a) 5 M and (b) 10 M.

3.2. Structural analysis

A typical XRD pattern of the as-prepared samples is shown in Fig. 3, and is similar to the presented by several researchers reporting on TiO_2 nanotubes [6,18,19,21,23–25,27–31,33–36,39,41]. Stengl et al. [49] presented XRD patterns similar to those shown in the present work: they used ethylene glycol as an agent in the synthesis of their products (a glycolate complex) and commercial sodium titanate as precursor. The diffraction lines of the glycolate complex are shown in the Table 2 for comparison. Fig. 3a shows the evolution of the XRD pattern in the treatment at 5 M as a function of the reaction time, confirming that at short reaction times only the surface of each particle is modified. This thin layer was detected by XPS, whereas the XRD pattern exhibited the anatase phase of the unreacted core of each particle. The diffraction lines corresponding to titanates appear after 2 days of reaction, as traces in the XRD pattern. However, three days of reaction are detrimental to the sample because the diffraction lines correspond (at least for this sample) to a less crystalline phase, eventually amorphous. This is not an unexpected behavior: Yoshimura et al. reported a loss of crystallinity in $BaTiO_3$ films on titanium foil after long hydrothermal treatments [50]. In our case, after a 6-day treatment the samples exhibited crystallinity again, completely transformed to the metastable phase, as shown in Fig. 3a.

Fig. 3b shows the evolution of the XRD pattern as a function of the reaction time in treatments at 10 M. The XRD pattern after a reaction time of 12 h presented coexistence of two phases, anatase and titanate. After 18 h of reaction time, only reflections from a titanate phase were detected. This phase was clearly present after 2 days of reaction. After two days of reaction, recrystallization of the anatase was observed as a trace in the XRD pattern. After 3 days, the diffractogram clearly showed the anatase reflections as broad peaks, attributed to the nanometric scale of the wires and flakes. However, after a 6-day reaction new reflections were detected, attributed to hydrogen titanate indicated as HT in the Figure. The XPS spectrum of this sample presented a very low content of Na. In order to confirm this finding, a new sample was prepared: 8 days at 130 °C; its XPS spectrum did not exhibit Na. Its XRD pattern was not assigned definitively to a crystalline structure of hydrogen titanate.

According to the available diffraction databases, there are several possibilities to fit the XRD lines of the as-prepared samples. They could correspond to $H_2Ti_3O_7$ (JCPDS 36-0654), $H_{0.7}Ti_{1.855}\square_{0.175}O_4 \cdot H_2O$ ($\square$ = vacancy), $H_2Ti_2O_5 \cdot H_2O$ (JCPDS 47-0124), $Na_2Ti_3O_7$ (JCPDS 31-1329), $Na_2Ti_3O_7 \cdot nH_2O$, $Na_2Ti_6O_{13}$ (JCPDS 73-1398), and $Na_2Ti_6O_{13} \cdot nH_2O$, as shown in Table 2. However, none of them provides a satisfactory fit to the experimental data. The reflections are broad and of low intensity. This can be due to the small dimensions of the nanostructures, to surface defects or to water incorporation in the matrix. Indeed, changes in lattice parameters due to hydrothermal treatments at different temperatures, attributed to the water content, have been already reported [51,52].

All samples in this work were washed with 0.1 M HCl, but this treatment was not able to eliminate the sodium from the samples completely , i.e., the ion exchange of Na^+ by H^+ was not efficient. Na in the samples was detected by XPS as well as EDX. The XPS estimate for the atomic percentages is 6% and 10% for 5 and 10 M treatments, respectively. They are in agreement with the atomic percentage of sodium hexatitanate; therefore it seems plausible that this sodium is part of the structure and not a NaOH residual. Du et al. [24] claimed that their tubes prepared in 10 M NaOH concentration correspond to $H_2Ti_3O_7$ because their simulated XRD patterns matched the experimental ones reasonably well. However, their EDX measurements showed sodium at 1.05 keV, which they attributed to NaOH residuals. Grimes et al. [21] reported the fabrication of TiO_2 tubes synthesized at 180 °C, with thermal stability up to 500 °C. However, their diffraction lines are also consistent with titanate formation.

Papp et al. [14] synthesized sodium trititanate and sodium hexatitanate by fusion reaction from stoichiometric

Table 2
Comparison of observed reflections from as-synthesized samples with literature results for nanotubes or nanowires of hydrogen titanate [35], lepidocrocite titanate [36], divalent salt titanate [34], sodium trititanate [37], and glycolate complex [14]

As-synthesized samples		$H_3Ti_3O_7$ (Ref. [35])		Lepidocrocite titanate [36]		$H_2Ti_2O_4(OH)_2$ [34]		$Na_2Ti_3O_7 \cdot nH_2O$ [37]		Glycolate [14]	
2θ	I/I_0	2θ	I/I_0	2θ	I/I_0	2θ	I/I_0	2θ	I/I_0	2θ	I/I_0
9.75		9.6		9.8		~9.8		~10		~10	
24.4		24.37		24.2		~24		~25		~24	
28.2		28.02		26.8		~28		~28		~28	
38.3		38.76		48.4		~48		~48		~48	
39.0		48.22		62.9		~62				~62	
39.6											
48.3											
49.4											
62.6											

weights of TiO_2 and Na_2CO_3 calcined at 800 °C during 20 h. After acid hydrolysis they obtained their protonated forms of sodium titanate. They concluded that the ion exchange of Na^+ by H^+ occur or does not occur depending on the starting phase: a 97% of sodium trititanate was transformed into $H_2Ti_3O_7$, but only a small amount of Na^+ in sodium hexatitanate was replaced by H^+. The ion exchange of Na^+ by H^+ in the present work was studied through the thermal stability of the samples treated under different synthesis conditions. All samples were calcined in air at temperatures of 200, 400 and 700 °C for 24 h. Fig. 4a shows the XRD patterns of a sample hydrothermally treated at 5 M for 6 days. After heat treatment at 200 °C the sample still exhibited the same reflections as before heating. The sample heated at 400 °C exhibited the diffraction lines of the anatase and metastable phases (indicated by T). The XRD pattern of the sample heated at 700 °C exhibited planes corresponding to anatase (marked A), rutile (R) and sodium hexatitanate phases. Similar results were reported by Yoshida et al. [38], who studied the effects of the synthesis conditions and heat treatment on the crystalline structure of ion exchanged titanate nanotubes. The XRD patterns of our samples after calcination indicated that the products were completely transformed to anatase, i.e., Na^+ was eliminated in the ion exchange process. However, after longer hydrothermal treatments, the Na^+ is forming part of the structure of the as-synthesized as well as the calcined samples.

Figs. 4b and c show the XRD patterns of samples synthesized at 10 M with hydrothermal reaction times of 12, 18 and 24 h, which were calcined at the same temperatures as before, namely 200, 400, and 700 °C. Exceptionally, the sample treated at 18 h was calcined at 500 °C. In the samples treated during 12 h and 24 h, the metastable phase was completely transformed to the anatase phase. Their diffractograms, shown in Fig. 4b, did not show reflections from rutile, brookite or others phases. On the other hand, the sample treated during 18 h was stable up to 400 °C and was transformed to sodium hexatitanate after calcination at 500 °C (Fig. 3c, top), which is mixed with anatase and rutile phases. Similar results were reported by Zhao et al. [53], who performed a study of the thermal stability of the as-prepared samples obtained from a modified hydrothermal treatment of TiO_2 in NaOH, using H_2O_2 as an oxidant. Their products were arrays of wires of a new compound, $Na_2Ti_6O_{13} \cdot xH_2O$ ($x \approx 4.2$), but their diffraction lines of the as-synthesized samples do not correspond to those found in our work. This phase is metastable and it disappears when the samples are calcined at temperatures higher than 150 °C.

In summary, calcination of the 5 M samples indicated that the TiO_2 matrix retains the highest amount of sodium

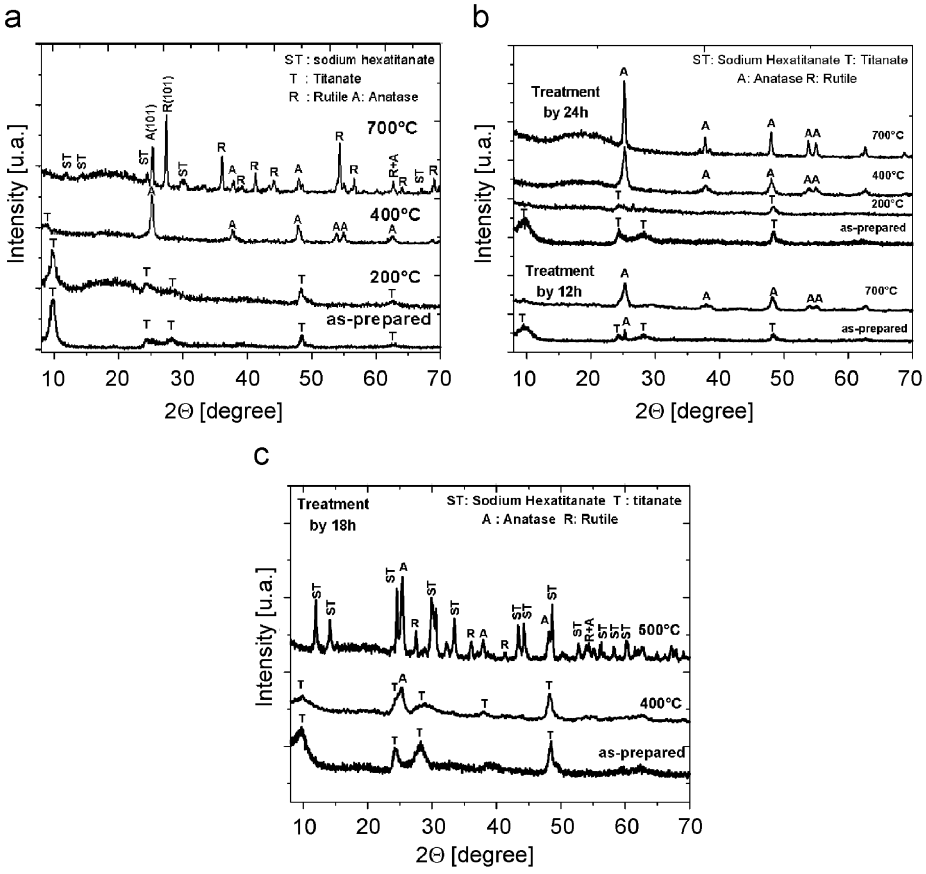

Fig. 4. XRD patterns of hydrothermal samples calcined at temperatures of 200, 400 and 700 °C. The synthesis conditions are the following: (a) at 5 M during 6-day; (b) at 10 M during 12 h and 24 h; and (c) 10 M during 18 h of reaction.

after a 6-day or longer hydrothermal treatment. However, maximum sodium retention in the 10 M samples is achieved after a 18-h hydrothermal treatment. All the 5 M and 10 M samples presented thermal stability up to 200 °C, except the sample treated at 10 M and 18 h of reaction time, as shown in Fig. 4. The synthesis of sodium titanate or titanium dioxide nanostructures involves a large amount of parameters. In the present work we remark that the duration of the hydrothermal reaction is critical for retaining the maximum Na atomic percentage.

Micro-Raman spectroscopy provides crystallographic information complementary to XRD. Fig. 5a shows Raman spectra of several samples as a function of treatment time and NaOH concentration. The top curves correspond to 10 M, and the bottom to 5 M. Curves labeled (a) correspond to a 1-day reaction, curves (b) to 3-day and curves (c) to 6-day reactions. Curve (a) with a 5 M NaOH concentration is the typical Raman spectrum of the anatase phase. Low NaOH concentrations and short reaction times do not allow the formation of a stable sodium titanate phase in the "bulk" (so Raman cannot detect it), since the phase transformation should begin at the surface of each particle. A 3-day hydrothermal treatment at the same NaOH concentration is detrimental to the samples, as revealed by the loss in Raman line sharpness. The broad Raman peaks and low intensity indicate a material of poor crystallinity or amorphous. As already mentioned this behavior has been previously observed in hydrothermal oxide films [50] and it is in agreement with our XRD results. Six days of reaction at the same NaOH concentration produce samples with clear vibration modes at 269, 285, 381, 445, 670, 703 and 824 cm^{-1} (see curve 4b, bottom). They possibly correspond to some metastable phase, but these vibration modes have not been yet definitively assigned to some crystalline structure or compound.

The samples treated in a 10 M NaOH concentration clearly exhibited the same vibration modes as the samples treated at 5 M, as shown in Fig. 5a (top curves). Such vibration modes do not correspond neither to TiO_2 phases (anatase, brookite or rutile) [22,54] nor to sodium tri or hexatitanate ($Na_2Ti_3O_7$ and $Na_2Ti_6O_{13}$) [14]. The 10 M-material hydrothermally treated during 6 days also exhibited broad Raman peaks with low intensity, indicating that the samples are composed of nearly amorphous material. Meng et al. [7] synthesized $Na_2Ti_6O_{13}$ nanowires and performed Raman measurements. Although the vibration modes exhibited in their samples were not definitively assigned to this compound, they concluded the existence of Na^+-O-Ti bonds. Gao et al. [23] prepared samples in a way similar to our work, and reported that their products were titanates identified as hydrate $H_2Ti_3O_7$, but their vibration modes correspond exactly to the Raman losses found in our study (see curves

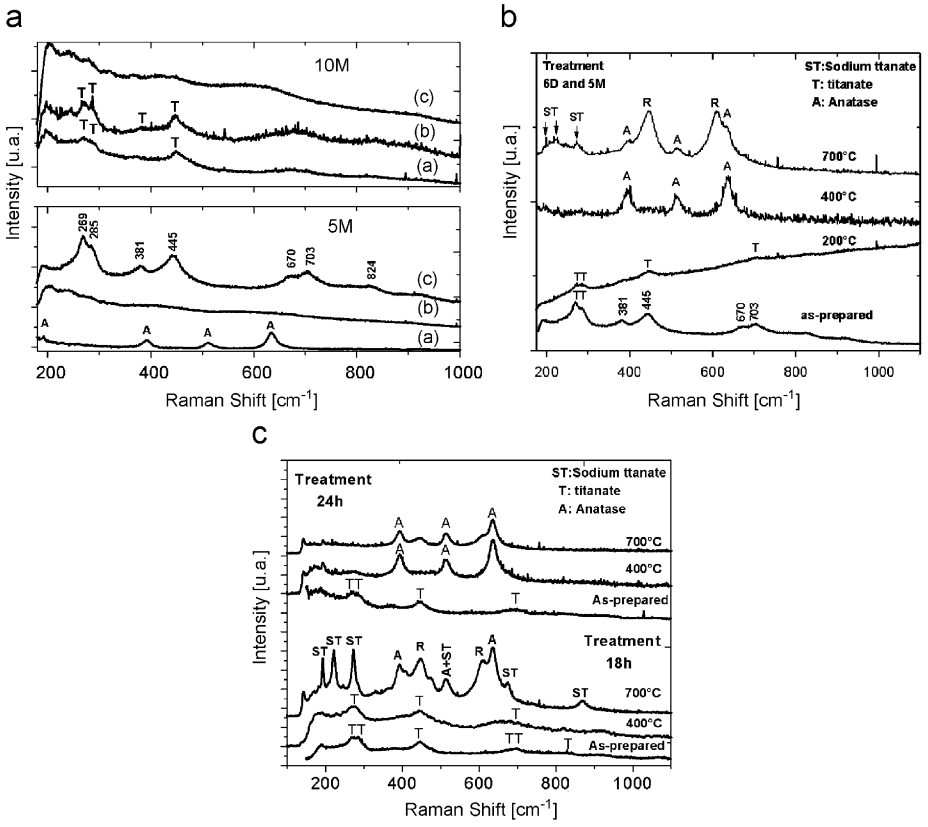

Fig. 5. Raman spectra of hydrothermal samples (a) as-synthesized at 5 M (bottom curves) and 10 M (top curves). Samples calcined at temperatures of 200, 400 and 700 °C: treatments at (b) 5 M during 6-day and (c) 10 M during 18 h and 24 h of reaction.

c at bottom in Fig. 4a). Our results indicate that the synthesized compounds should be identified as some phase of sodium titanate, in agreement with the XPS, XRD and EDX analyses.

Thermal stability was also investigated using Raman spectroscopy. Fig. 5b shows Raman shifts of a sample treated at 5 M for 6 days and calcined in air at 200, 400 and 700 °C. At 200 °C the sample still exhibits the phase of the as-synthesized samples, but the form of the curve at 200 °C represents fluorescence emission. At 400 °C the sample exhibited a complete phase transformation from sodium titanate to anatase phase. The Raman spectrum of the sample calcined at 700 °C exhibited vibration modes of anatase (marked A), rutile (marked R) and sodium hexatitanate phases (marked ST and indexed as $Na_2Ti_6O_{13}$). Fig. 5c shows Raman loss of a sample hydrothermally treated for 18 and 24 h in 10 M NaOH concentration. In the case of the sample synthesized by 18 h, thermal stability extends to temperatures higher than 400 °C, and the Raman spectrum of the sample calcined at 700 °C exhibited vibration modes of sodium hexatitanate mixed with Raman lines corresponding to the anatase and rutile phases. The sample treated during 24 h was stable up to temperatures higher then 200 °C; at 700 °C the sample was transformed to anatase completely. In summary, the thermal stability of the samples indicated that the matrix can retain high amounts of sodium after 6-day or longer hydrothermal treatments at 5 M, and after only 18 h at 10 M.

3.3. Microstructural analysis

Fig. 6a is a SEM micrograph of the as-synthesized samples treated at 5 M and 1 day of reaction. The oxide exhibits a belt-like structure 8 to 40 nm in width and from 100 nm to several micrometers in length. The surface of each particle is completely composed of sodium titanate nanobelts, but the center of the particles is composed of unreacted material, as shown in Fig. 6b. This low magnification TEM image shows particles and lamellar and beltlike structures. The features observed in this micrograph agree with the work of Grimes et al. [21], who collected material before the completion of the hydrothermal reaction, finding lamellar structures.

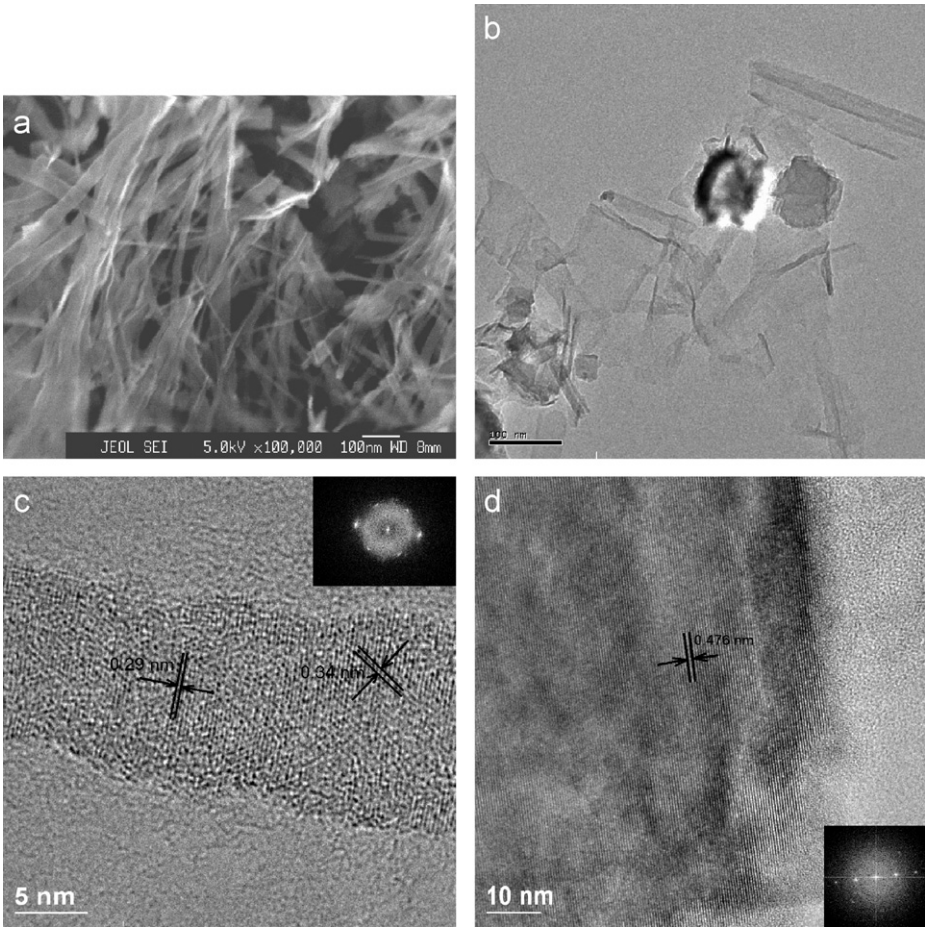

Fig. 6. SEM and TEM micrographs of the samples prepared hydrothermally at 5 M by 1 day at 130 °C: (a) SEM image of sodium titanate nanobelt structures; (b) low magnification TEM image showing particles and lamellar and beltlike structures; (c) HRTEM image of a nanobelt showing two set of fringes along [−3 1 1] and [−1 1 1] directions of $Na_2Ti_6O_{13}$; and (d) enlarged image of a particle of Fig. 6c showing the distance between fringes attributed to anatase.

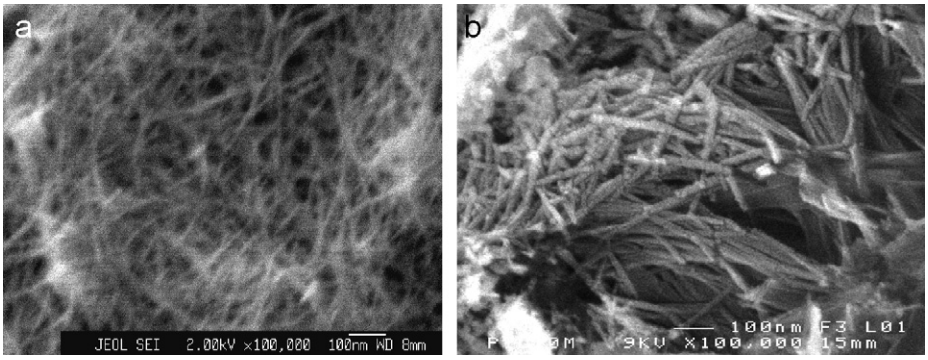

Fig. 7. FEG-SEM images of samples treated at 10 M, (a) 18 h of reaction and (b) 1 day of reaction.

A HRTEM image of a tubular structure synthesized at 5 M and 1 day of reaction, shown in Fig. 6c, reveals two sets of planes with separations of 0.29 and 0.34 nm, which could correspond to the interplanar distances of the (−3 1 1) and (−1 1 1) planes in $Na_2Ti_6O_{13}$, respectively. These values could also correspond to the (−2 0 2) and (0 1 2) interplanar distances in $Na_2Ti_3O_7$, or also to the (1 2 1) and (1 1 1) planes of TiO_2 in the brookite phase. We discard the latter because of the sodium content revealed by XPS in the 5 M samples. However, none of the planes and compounds assigned provides a satisfactory fit to the experimental data. Moreover, none of them represents planes of high symmetry of sodium tri-hexatitanate or brookite phases. The top inset in Fig. 6c is the two-dimensional Fourier transform, which indicated two set of planes. Fig. 6d shows the HRTEM image of one of the particles identified in Fig. 6b, with planes separated 0.476 nm, corresponding to the interplanar (0 0 2) distance in anatase. The bottom inset of the Fig. 6d is the two-dimensional Fourier transform corresponding to the (0 0 2) plane of a anatase particle.

Fig. 7 shows SEM micrographs of hydrothermal samples prepared in 10 M NaOH. Fig. 7a corresponds to a sample prepared at 130 °C for 18 h, showing wire-like structures with diameters from 8 up to 10 nm with minimal dispersion, and lengths of several μm. Fig. 7b corresponds to the sample prepared at 130 °C for 1-day, exhibiting wires and rods with diameters from 7 to 40 nm and lengths from 100 to several micrometers. Treatments with short reaction time lead to long wire-like structures, while at longer reaction times the wires seem to break into rods.

4. Conclusions

A hydrothermal treatment of fine TiO_2 particles at 130 °C under alkali conditions leads to sodium titanate belt-like and wire-like structures, at NaOH concentrations of 5 and 10 M, respectively. This claim is supported by measurements performed with redundant complementary analytical techniques: X-ray photoelectron spectroscopy (XPS) and energy dispersive X-ray spectroscopy (EDX), Raman spectroscopy and X-ray diffraction, scanning electron microscopy (SEM) and transmission electron microscopy (TEM).

An interesting feature of our study is that the belt-like and wire-like structures underwent a phase transformation from anatase to sodium titanate, most probably a metastable phase. XPS measurements are consistent with the existence of Na^+-O-Ti bonds on the surface of all hydrothermal samples, even when they were prepared at low concentrations and short reaction times. In this case, XRD and Raman spectroscopy analyses indicated that these samples exhibited the anatase phase in the bulk, confirming that the reaction starts on the surface of each particle. At longer reaction times, XRD and Raman spectroscopy confirmed the presence of mainly one phase of sodium titanate, compound that has not been indexed yet. The thermal stability study of the samples indicated that the sodium titanate is a metastable phase up to temperatures higher than 200 or 400 °C depending on the sodium content. In the present work we remark that the duration of the hydrothermal reaction is critical: the retention of sodium in the matrix is essential for the synthesis of titanium dioxide or sodium titanate nanostructures.

Acknowledgments

This work was partially supported by the DGIP of the Universidad Católica del Norte. We acknowledge Prof. D. Ugarte, at the Laboratorio Nacional de Luz de Sincrotron (LNLS), Campinas, who allowed us to use FEG-SEM and TEM facilities. Also, we acknowledge to Dr. Jaime Llanos who allowed us to use the facilities of the Inorganic Laboratory, Departamento de Ciencias Químicas y Farmacéuticas. We acknowledge to Mr. Andrés Ibáñez for recording the XRD patterns. V.M.F. acknowledges grant FONDECYT 1040954. A.Z.A. acknowledges grant FUNDACIÓN ANDES under contract No. C-13876. We thank Dr. Boris Chornik for the great kindness in reading the manuscript.

References

[1] R. Saito, M. Fujita, G. Dresselhaus, M. Dreselhaus, Physical Properties of CarbonNanotubes, Imperial College Press, 1998;
R. Saito, M. Fujita, G. Dresselhaus, M. Dreselhaus, Appl. Phys. Lett. 60 (1992) 2204.

[2] K. Varghese, C. Grimes, J. Nanosci. Nanotechnol. (4) (2003) 277.

[3] G.R. Patzke, F. Krumeich, R. Nesper, Angew. Chem. Int. 41 (2002) 2446.

[4] X. Sun, X. Chen, Y. Li, Inorganic Chem. 41 (2002) 4996.

[5] A.L. Sauvet, S. Baliteau, C. Lopez, P. Fabry, J. Solid State Chem. 177 (2004) 4508.

[6] C. Zhang, X. Jiang , A. Tian, B. Tian, X. Wang, X. Zhang, Z. Du, Colloids Sur. A Physicochem. Eng. Aspects 257–58 (2005) 521.

[7] X. Meng, D. Wang, J. Liu, S. Zhang, Mater. Res. Bull. 39 (2004) 2163.

[8] D.J. Corcoran, D.P. Tunstall, J.T. Irvine, Solid State Ionics 297 (2000) 136.

[9] I.M. El-Nagar, E.A. Mowafy, I.M. Ali, H.F. Aly, Adsorption 8 (3) (2002) 225.

[10] R.D. Adams, R. Layland, M. Danot, C. Payen, PolyHedron 15 (1996) 2567.

[11] J. Maier, M. Holzinger, W. Sitte, Solid State Ionics 74 (1994) 5–9.

[12] H.J. Maier, W. Sitte, Solid State Ionics 86–88 (1996) 1055–1062.

[13] J. Ramirez-Salgado, P. Fabry, Sensors and Actuators B Chemical 82 (2002) 34;
J. Ramirez-Salgado, E.D. Jurado, P. Fabry, J. Eur. Ceram. Soc. 24 (2004) 2477.

[14] S. Papp, L. Korosi, V. Meynen, P. Cool, E. Vansant, I. Dekany, J. Solid State Phys. 178 (2005) 1614.

[15] T. Kasuga, M. Hiramatsu, A. Hoson, T. Sekino, K. Niihara, Langmuir 14 (1998) 3160.

[16] Y. Kolen'ko, K. Kovnir, A. Gavrilov, A. Garshev, J. Frantti, O. Lebedev, B. Churagulov, G. Tendeloo, M. Yoshimura, J. Phys. Chem. B 110 (2006) 4030.

[17] Y.Q. Wang, G.Q. Hu, X.F. Duan, H.L. Sun, Q.K. Xue, Chem. Phys. Lett. 365 (2002) 427.

[18] S. Zhang, J. Zhou, Z. Zhang, Z. Du, A. Vorontsov, J. Zhensheng, Chin. Sci. Bull. 45 (16) (2000) 1533.

[19] Z. Yuan, B. Su, Colloids Surfaces A Physicochem. Eng. Aspects (2004) 173; Z. Yuan, J. Colomer, B. Su, Chem. Phys. Lett. 363 (2002) 362.

[20] L. Kavan, M. Kalbac, M. Zukalova, I. Exnar, V. Lorenzen, R. Nesper, M. Greatzel, Chem. Mater. 16 (2004) 477.

[21] W. Wang, O. Varghese, M. Paulose, C. Grimes, J. Mater. Res. (2) (2004) 417.

[22] I. Park, S. Jang, J. Hong, R. Vittal, K. Kim, Chem. Mater. (2003) 4633.

[23] X. Gao, H. Zhu, G. Pan, S. Ye, Y. Lan, F. Wu, D. Song, J. Phys. Chem. B 108 (2004) 2868.

[24] G. Du, Q. Chen, R. Che, Z. Yuan, L. Peng, Appl. Phys. Lett. 79 (22) (2001) 3702;
Q. Chen, W. Zhou, G. Du, L. Peng, Adv. Mater. 14 (2002) 1208.

[25] D. Wu, J. Liu, X. Zhao, A. Li, Y. Chen, N. Ming, Chem. Mater. 18 (2006) 547.

[26] Z. Tian, J. Voigt, J. Liu, B. Mchenzie, H. Xu, J. Am. Chem. Soc. 125 (2003).

[27] J. Li, Z. Tang, Z. Zhang, Chem. Mater. 17 (2005) 5848;
J. Li, Z. Tang, Z. Zhang, Electrochem. Solid State Lett. 8 (11) (2005) A570.

[28] H. Zhu, X. Gao, Y. Lan, D. Song, Y. Xi, J. Zhao, J. Am. Chem. Soc. (2004) 8380; H. Zhu, Y. Lan, X.P. Gao, S.P. Ringer, Z.F. Zheng, D. Song, J.C. Zhao, J. Am. Chem. Soc. (2004) 6730.

[29] D. Wu, Y. Chen, N. Ming, Appl. Phys. Lett. 87 (2005) 112501;
D. Bavykin, A. Lapkin, P. Plucinski, J. Freidrich, F. Walsh, J. Phys. Chem. 109 (2005) 19422.

[30] L. Qian, Z.S. Jin, J.W. Zhang, Y.B. Huang, Z.J. Zhang, Z. Du, Appl. Phys. A Mater. Sci. Process. (2004) 12384.

[31] J. Yang, Z. Jin, X. Wang, W. Li, J. Zhang, S. Zhang, Dalton Trans. (2003) 3898.

[32] M. Zhang, Z. Jin, J. Zhang, X. Guo, J. Yang, W. Li, X. Wang, S. Zhang, J. Mol. Catal. A Chem. 217 (2004) 203.

[33] J. Nian, H. Teng, J. Phys. Chem. 110 (2006) 4193.

[34] C. Tsai, H. Teng, Chem. Mater. 18 (2006) 367.

[35] Y. Mao, M. Kanungo, T. Henraj-Benny, S. Wong, J. Phys. Chem. 110 (2006) 702.

[36] R. Ma, K. Fukuda, T. Sasaki, M. Osada, Y. Bando, J. Phys. Chem. B 109 (2005) 6210;
R. Ma, T. Sasaki, Y. Bando, J. Am. Chem. Soc. 126 (2004) 10382;
R. Ma, Y. Bando, T. Sasaki, J. Phys. Chem. 108 (2004) 2115;
T. Sasaki, R. Ma, S. Nakano, S. Yamauchi, M. Watanabe, Chem. Mater. 9 (1997) 602–608.

[37] O. Ferreira, A. Souza, J. Mendes, O. Alves, J. Braz. Chem. Soc. 17 (2) (2006) 393.

[38] R. Yoshida, Y. Suzuki, S. Yoshikawa, Materials Chemistry and Physics 91 (2005) 409.

[39] B. Poudel, W. Wang, C. Dames, J. Huang, S. Kunwar, D. Wang, D. Barnerjee, G. Chen, Z. Ren, Nanotechnology 16 (2005) 1935.

[40] D. Seo, H. Kim, J. Lee, J. Crystal Growth 275 (2005) e2371.

[41] M. Wei, Y. Konishi, H. Zhou, H. Sugihara, H. Arakawa, Solid State Commun. 133 (2005) 493.

[42] A. Kukovecz, M. Hodos, E. Horvath, G. Radnoczi, Z. Konya, I. Kiricsi, J. Phys. Chem. B Lett. 109 (2005) 17781.

[43] Q. Li, P. Harter, W. Xue, J. Zuo, W. Herrmann, J. Chem. Soc. Dalton Trans. (2001) 2719.

[44] M. Khan, H. Jung, O. Yang, J. Phys. Chem. B 110 (13) (2006) 6626–6630.

[45] E. Pabón, J. Retuert, R. Quijada, A. Zárate, Microporous Mesoporous Mater. (2004) 195.

[46] J. Moulder, W. Sticke, P. Sobol, K. Bomben, in: J. Chastain (Ed.), Handbook of X-ray Photoelectron Spectroscopy, Perkin Elmer Corporation, Physical Electronics Division, USA, 1992.

[47] R. Reiche, D. Dobler, J.P. Holgado, A. Barranco, A.I. Martín-Concepción, F. Yubero, J.P. Espinós, A.R. González-Elipe, Surf. Sci. 537 (2003) 228.

[48] S. Oswald S, A.R. González-Elipe, R. Reiche, J.P. Espinós, A. Martin, Surf. Interface Anal. 35 (2003) 991.

[49] V. Stengl, S. Bakardjiieva, J. Subrt, E. Vecernikova, L. Szartmary, M. Klementova, V. Balek, Appl. Catal. B Environmental 63 (2005) 20.

[50] S.E. Yoo, M. Hayashi, M. Yoshimura, M. Hayashi, N. Ishizawa, Jpn. J. Appl. Phys. Part 2 28 (1989) L2007.

[51] C.T. Xia, E.W. Shi, W.Z. Zhong, J.K. Guo, J. Crystal Growth 166 (1–4) (1996) 961.

[52] J. Lisoni, F. Piera, M. Sanchez, C. Soto, V. Fuenzalida, Appl. Surf. Sci. 134 (1–4) (1998) 225.

[53] Y. Zhao, U.H. Lee, M. Suh, Y.U. Kwon, Bull. Korean Chem. Soc. (9) (2004) 1341.

[54] Y.H. Zhang, C.K. Chan, J.F. Porter, W. Guo, J. Mater. Res. (9) (1998) 2602.

[55] A. Barrie, F.J. Street, J. Electron Spectrosc. Relat. Phenom. 7 (1977) 1.